

## Elastic electron scattering from 3-hydroxytetrahydrofuran: experimental and theoretical studies

V Vizcaino<sup>1</sup>, J Roberts<sup>1,2</sup>, J P Sullivan<sup>1</sup>, M J Brunger<sup>2</sup>,  
S J Buckman<sup>1</sup>, C Winstead<sup>3</sup> and V McKoy<sup>3</sup>

<sup>1</sup> Centre for Antimatter-Matter Studies, AMPL, RSPHysSE,  
Australian National University, 0200 Canberra, Australia

<sup>2</sup> Centre for Antimatter-Matter Studies, SOCPES, Flinders University,  
GPO Box 2100, Adelaide 5001, South Australia

<sup>3</sup> A A Noyes Laboratory of Chemical Physics, California Institute of  
Technology, Pasadena, CA 91125, USA

E-mail: [Stephen.buckman@anu.edu.au](mailto:Stephen.buckman@anu.edu.au) and [carl@schwinger.caltech.edu](mailto:carl@schwinger.caltech.edu)

*New Journal of Physics* **10** (2008) 053002 (10pp)

Received 04 March 2008

Published 6 May 2008

Online at <http://www.njp.org/>

doi:10.1088/1367-2630/10/5/053002

**Abstract.** We report the results of measurements and calculations for elastic electron scattering from 3-hydroxytetrahydrofuran ( $C_4H_8O_2$ ). The measurements are performed with a crossed electron-target beam apparatus and the absolute cross-sections are determined using the relative flow technique. The calculations are carried out using the Schwinger multichannel method in the static-exchange plus polarization (SEP) approximation. A set of angular differential cross-sections (DCS) is provided at five incident energies (6.5, 8, 10, 15 and 20 eV) over an angular range of 20–130°, and the energy dependence of the elastic DCS at a scattering angle of 120° is also presented. Integral elastic and elastic momentum transfer cross-sections have also been derived and calculated. The results are compared with those of recent measurements and calculations for the structurally similar molecule tetrahydrofuran ( $C_4H_8O$ ).

**Contents**

<b>1. Introduction</b>	<b>2</b>
<b>2. Experimental apparatus and techniques</b>	<b>2</b>
<b>3. Theoretical calculations</b>	<b>4</b>
<b>4. Results and discussion</b>	<b>4</b>
4.1. Elastic DCS . . . . .	4
4.2. Energy dependence of the elastic DCS . . . . .	7
4.3. Integral and momentum transfer cross-section . . . . .	8
<b>5. Conclusions</b>	<b>9</b>
<b>Acknowledgments</b>	<b>9</b>
<b>References</b>	<b>10</b>

**1. Introduction**

Electron interactions with biomolecules have been the subject of considerable interest since it was discovered that low energy electrons can cause significant DNA strand damage [1]. Electrons readily attach at specific energies to the molecular constituents of DNA to form transient negative ions, which then can dissociate to produce free radicals. This bond breaking process, called dissociative electron attachment (DEA), has been demonstrated in numerous molecules such as water, DNA bases, amino acids and fluorocarbons.

The present paper on electron scattering from 3-hydroxytetrahydrofuran (3-hTHF) follows recent experimental [2]–[7] and theoretical [8]–[11] studies on tetrahydrofuran (THF). Both of these molecules have similar structures, and 3-hTHF is another common analogue to the deoxyribose sugar component in DNA (see figure 1). DEA studies [2] have shown, on both molecules, the presence of a resonance at around 6.2 eV, which decays through a number of means, one of which (DEA) causes the molecule to dissociate, leading to the loss of a hydrogen atom. The DEA cross-section for 3-hTHF is around 30 times greater than that for THF, and this is thought to be due to the presence of the OH group. The OH group also results in 3-hTHF having several low energy conformers with low barriers against rotation.

To our knowledge, there are no other data available in the literature on electron scattering cross-sections for 3-hTHF. This paper provides the first absolute differential cross-section measurements and calculations on elastic scattering from 3-hTHF.

**2. Experimental apparatus and techniques**

Elastic electron scattering from 3-hTHF has been studied using a crossed electron-target beam apparatus [12]. 3-hTHF poses some particularly difficult experimental problems as it has a very low vapor pressure at room temperature (less than 1 Torr), as opposed to THF, which has a vapor pressure in excess of 140 Torr at that temperature. Therefore, the gas-handling system (gas source, gas lines, needle and shut-off valves, Baratron gauge) had to be uniformly heated at 90 °C to produce a stable driving pressure for the molecular beam. The beam-forming needle, through which the gas enters the collision region, is also held at 90 °C. At that temperature the vapor pressure above the liquid sample is typically 20 Torr. However, the elevated temperature

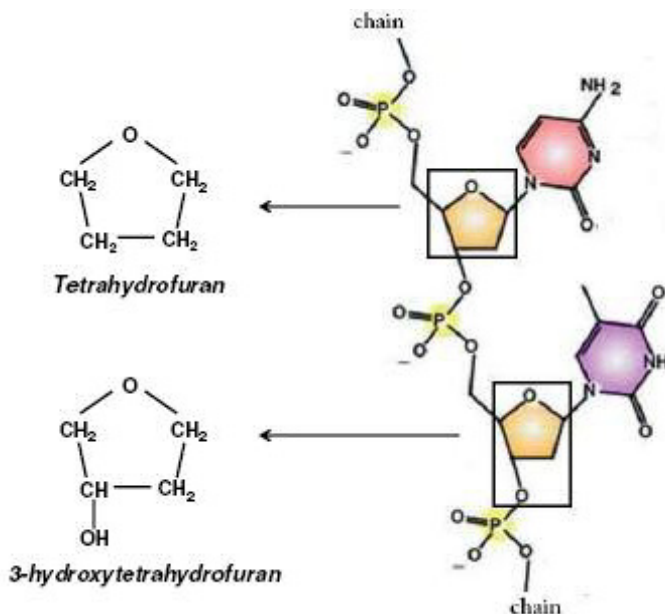


**Figure 1.** Single strand of DNA with the two common analogues for the deoxyribose ring: THF molecule, and the 3-hTHF molecule.

also means that the beam will contain a significant fraction of rotationally and vibrationally excited species. 3-hTHF has 36 vibrational modes, many of which have small excitation energies, and a simple calculation assuming a Boltzmann distribution, and considering only the vibrational states of 3-hTHF, shows that at 90 °C less than 30% of the molecular beam will be in the ground vibrational state. 3-hTHF also has several conformers that lie at low energies and which might be populated in a hot, thermal beam such as that used for the present measurements. Unfortunately this situation cannot be avoided for an effusive beam of 3-hTHF and it should be kept in mind when interpreting the results we present in section 4.

The electron beam is obtained from a conventional electron monochromator with reasonable energy resolution (FWHM around 60 meV) and scattered electrons are energy analyzed before being detected by a channel electron multiplier. The analyzer is mounted on a turntable allowing the measurement of DCS in the angular range from 20° to 130°. The absolute value of the incident energy was determined through calibration against the position of the  $1s2s^2\ ^2S$  negative ion resonance feature for electron scattering from helium at 19.365 eV [13] or the position of the quasi-vibrational resonance peaks in the  $^2\Pi_g$  shape resonance in  $N_2$  [14].

Absolute cross-sections are determined using the relative flow technique [15]. This involves the measurement of the relative electron scattering intensities for the gas under study (3-hTHF) and helium, for which there is an accurate set of DCS. The He cross-section established by Nesbet [16] is employed as the standard in the present work with the exception of the 20 eV measurement where the tabulated cross-sections of Boesten and Tanaka [17] have been used. The driving pressures for both gases are determined in such a way that their collisional mean-free-paths are the same in the beam-forming capillary. This is done in order to minimize the effects that collisions have on the relative shapes of the atomic and molecular beams. Typical driving pressures used were 0.19 Torr (3-hTHF) and 1 Torr (He). Despite the efforts made to keep the driving pressure as stable as possible by heating the gas lines and the needle

valve, the behavior of 3-hTHF was quite unpredictable. This was thought to be due to the partial condensation occurring at critical parts of the gas lines, such as the needle valve, and the subsequent release of a burst of gas when these condensates or bubbles broke free. The significant pressure fluctuations that resulted had to be closely monitored, and accounted for, during data accumulation.

### 3. Theoretical calculations

The geometry of 3-hTHF was optimized at the level of second-order Möller–Plesset perturbation theory using the electronic structure package GAMESS [18] and the 6–31G(*d*) basis set as contained therein. The result is an ‘envelope’ structure in which C<sub>1</sub>, C<sub>2</sub>, C<sub>3</sub> and the ring oxygen are approximately planar, while C<sub>4</sub> is bent to the opposite side of the ring from the OH group, which is oriented axially (C<sub>1</sub>–C<sub>2</sub>–C<sub>3</sub>–O<sub>3</sub> dihedral angle  $-85.9^\circ$ ) with the hydrogen pointed toward the ring oxygen, indicative of an internal hydrogen bond. Berthier *et al* [19] and Giardini *et al* [20] found similar structures for the lowest-energy conformer. The ground-state Hartree–Fock wave function was computed at the optimized geometry within the triple-zeta valence (TZV) basis set as contained in GAMESS, with a 3d polarization and 1s1p diffuse supplement on the heavy atoms and a 2p polarization and 1s diffuse supplement on the hydrogens; GAMESS’s default exponents and splitting factors were used for the supplemental functions, and  $x^2 + y^2 + z^2$  linear combinations of Cartesian d orbitals were excluded. The Hartree–Fock virtual orbitals were transformed into modified virtual orbitals (MVOs) [21] using a +6 cationic Fock operator. Scattering calculations were carried out using the Schwinger multichannel (SMC) method [22, 23] as implemented for parallel computers [24]. All 254 MVOs were coupled with the Hartree–Fock ground state to form the open-channel part of the variational space for the SMC calculation. To describe polarization effects, singlet excitations from the 7 most tightly bound valence orbitals into the 10 MVOs with lowest energy were coupled with the 50 lowest MVOs to form doublet closed-channel terms included in the variational space, while for the 7 outermost valence orbitals, we included singlet excitations into the 18 lowest MVOs coupled with the lowest 100 MVOs to form doublet configurations. The dimension of the resulting variational space was 14 968. On the whole, the 3-hTHF scattering calculation is similar in design to that done for THF [8], which yielded good results; however, the absence of symmetry in 3-hTHF required a less extensive treatment of polarization.

## 4. Results and discussion

### 4.1. Elastic DCS

Absolute DCS for elastic electron scattering from 3-hTHF are presented in table 1, and shown graphically in figure 2, where we also compare with the present calculations and our previous measurements and calculations for THF.

In general, we can see from the various panels of figures 2(a)–(e) that the shape and magnitude of the cross-sections are quite similar for both 3-hTHF and THF. While the calculation suggests that 3-hTHF has a slightly larger cross-section than THF, the experimental data however seem to show the contrary. This is especially the case at forward and backward angles where the 3-hTHF cross-section is systematically smaller, a tendency which increases

**Table 1.** Absolute DCS for elastic scattering from 3-hTHF, in units of  $10^{-16} \text{ cm}^2 \text{ sr}^{-1}$ . The uncertainty is given in parentheses (%). The ICS and MTCS for each incident energy are given in units of  $10^{-16} \text{ cm}^2$  at the base of each column and the uncertainty on this value is estimated to be around 20%.

Angle	Incident energy (eV)				
	6.5	8	10	15	20
20	7.25 (7.41)	7.74 (9.12)	12.79 (8.31)	11.28 (7.96)	21.34 (7.85)
25	5.22 (7.26)	5.67 (8.57)	—	6.26 (7.38)	—
30	3.59 (7.69)	3.85 (7.54)	5.05 (8.36)	3.59 (7.58)	5.02 (7.23)
40	2.46 (7.84)	2.18 (8.38)	2.55 (8.51)	2.05 (7.66)	2.10 (7.51)
50	1.83 (8.26)	1.64 (7.57)	1.88 (7.74)	1.72 (7.83)	1.59 (14.8)
60	1.63 (7.26)	1.41 (7.74)	1.51 (7.34)	1.48 (7.38)	1.45 (7.67)
70	1.42 (7.26)	1.37 (7.46)	1.32 (7.22)	1.32 (7.50)	1.23 (8.10)
80	1.42 (7.22)	1.38 (7.23)	1.29 (7.45)	1.23 (7.52)	1.05 (8.31)
90	1.56 (7.29)	1.49 (7.38)	1.38 (7.38)	1.31 (7.39)	1.01 (10.7)
100	1.82 (7.47)	1.70 (7.21)	1.47 (7.35)	1.34 (7.22)	0.95 (7.89)
110	2.09 (7.25)	1.87 (7.51)	1.51 (7.39)	1.36 (7.44)	0.93 (8.91)
120	2.21 (7.26)	2.12 (7.53)	1.71 (7.39)	1.39 (7.35)	1.06 (10.5)
130	2.36 (7.37)	2.19 (7.39)	1.85 (7.47)	1.40 (7.43)	1.26 (8.24)
ICS	30.6	26.7	30.4	28.6	32.7
MTCS	27.0	22.3	21.4	20.7	18.0

as the incident energy decreases. Indeed for a scattering angle of  $30^\circ$ , the cross-sections for the two gases differ only by 1% at 20 eV (figure 2(e)) but by 40% at 6.5 eV (figure 2(a)).

Before discussing these differences and the possible reasons for them, it is prudent to consider that the present measurements on 3-hTHF were only possible after heating the sample and gas handling system to  $90^\circ\text{C}$ . The liquid sample of this molecule was quite sugar-like in its consistency and the vapor pressure at room temperature was less than 1 Torr. By heating to  $90^\circ\text{C}$ , we were able to raise the vapor pressure to about 20 Torr but, as we have already mentioned, this meant that only about 30% of the molecules in the interaction region would have been in the ground vibrational level. Also, as discussed above, several possible conformers of 3-hTHF would also be present in a hot molecular beam. This is quite different to the situation for THF and this initial vibrational/conformer distribution could possibly be the cause for some of the observed differences.

With that caveat, a first approach to explaining the relative behavior of the DCS at forward angles is to consider the dipole moments and dipole polarizabilities of the two molecules. In general one can expect a larger dipole moment and/or dipole polarizability to result in a larger cross-section at forward angles and lower energies. An experimental determination of the dipole moment of THF suggests a value of 1.63 Debye [25], while for 3-hTHF, the only experimental value in the literature is 1.67 Debye [26]—i.e. there is little difference between the two. As discussed, 3-hTHF has several conformers that lie at low energies and which might be populated in a hot beam such as that used for the present measurements. Calculations of the dipole moments for these different structures, using the Gaussian package, reveal quite different values. The lowest lying (ground state) conformer has a dipole moment of 1.74 Debye, the first

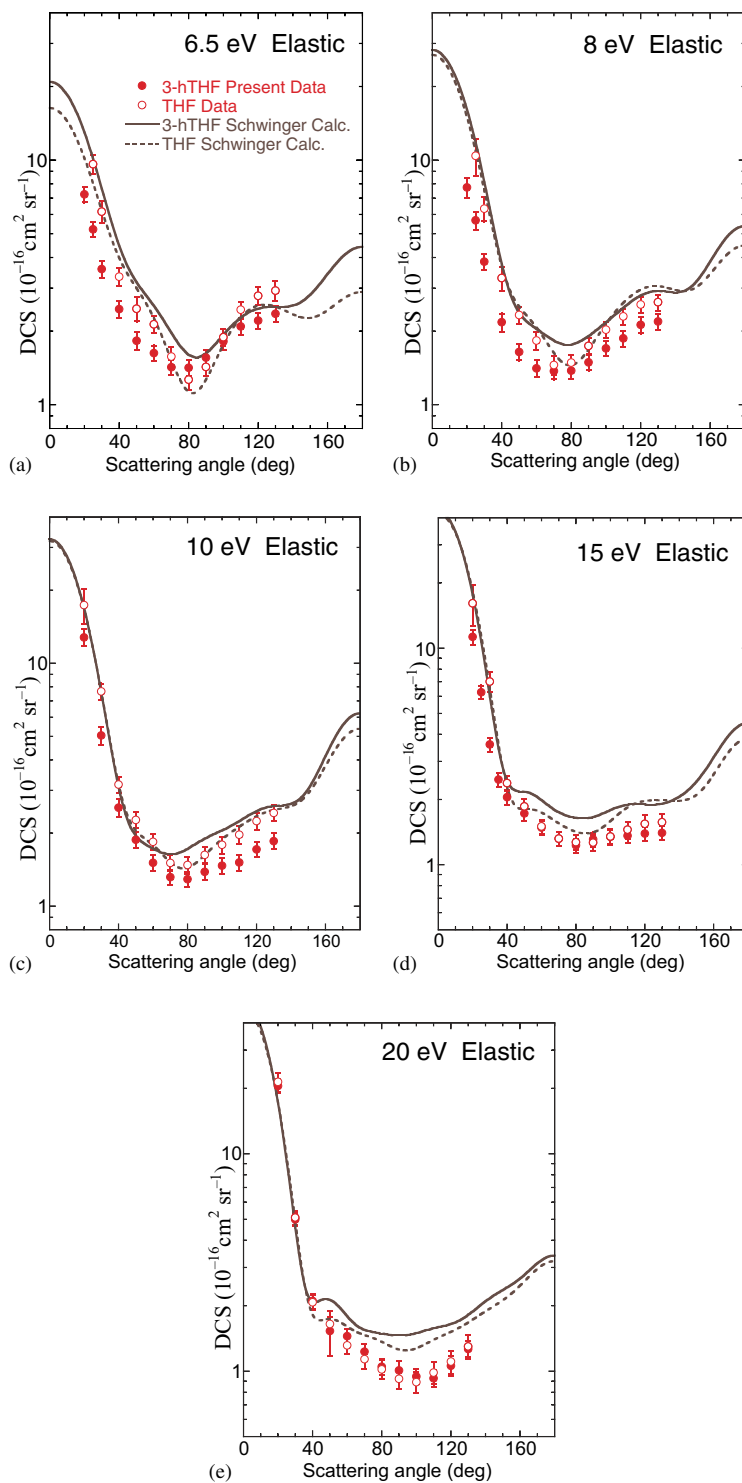


**Figure 2.** Absolute DCS ( $10^{-16} \text{ cm}^2 \text{ sr}^{-1}$ ) for elastic electron scattering from 3-hTHF at: (a) 6.5 eV, (b) 8 eV, (c) 10 eV, (d) 15 eV and (e) 20 eV. The experimental measurements are shown as full circles for 3-hTHF and open circles for THF, the Schwinger calculations as a full line for 3-hTHF and a broken line for THF.

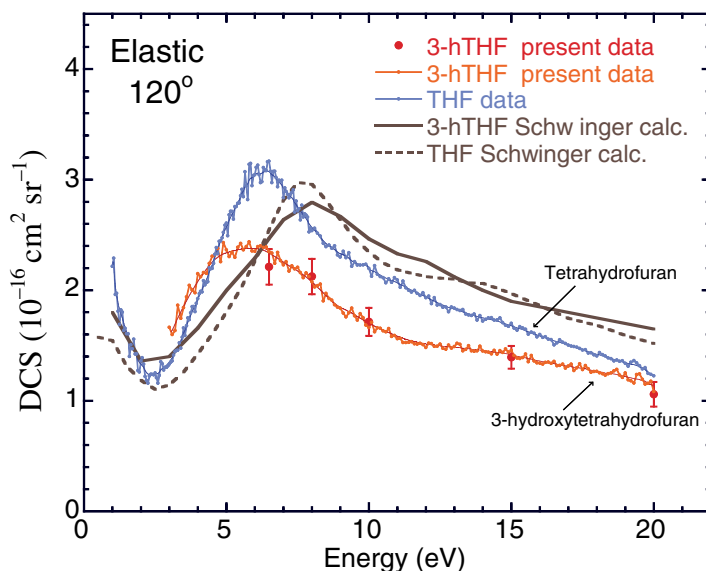


**Figure 3.** Absolute DCS ( $10^{-16} \text{ cm}^2 \text{ sr}^{-1}$ ) shown as a function of energy at a scattering angle of  $120^\circ$ . See legend on figure and text for further details.

rotational conformer a value of 2.87 Debye and the third a value of 1.14 Debye. On the other hand, the calculated values of the dipole polarizabilities reveal little variation between THF and the various conformers of 3-hTHF, with all having the values of around 50 au.

Based on considerations of dipole moment and polarizability alone, it is thus not expected that one would see substantial differences between the scattering cross-sections for these two molecules and in fact that the cross sections for 3-hTHF might be larger than those for THF. This is indeed the case in the calculated values but not in the experiment, although the differences are not great. That the experimental elastic DCS for 3-hTHF appear to be generally a little lower than those for THF, at the same electron energy, is not consistent with the dipole moment calculations for the conformers. However, the possible effect of the presence of different vibrationally excited species in the beam is somewhat more difficult to predict.

#### 4.2. Energy dependence of the elastic DCS

In figure 3, we show the energy dependence of the elastic DCS over an energy range from 3 to 20 eV and at a fixed scattering angle of  $120^\circ$ . At this angle for THF, the cross-section shows a maximum at around 6.2 eV, which previous studies, including our own, have concluded is due to the presence of a negative ion resonance. Studies on vibrational excitation [7] and DEA [2] have both confirmed a resonance at that energy. The 3-hTHF cross-section also shows a maximum at around 6 eV but the feature is broader ( $\sim 4$  eV wide) and the magnitude, at least at this scattering angle, is generally lower. The Schwinger variational calculation shows a similar relative-energy dependence, but the features are shifted by about 2 eV to a higher energy (8 eV). These results indicate that the same resonance as observed in THF is also present in 3-hTHF, which is perhaps not a surprising result. Also shown on this figure are the angular DCS results at each of the five energies and an angle of  $120^\circ$  (as discussed above). These results are collected in a different experiment with the spectrometer in a completely different operational mode (angular versus

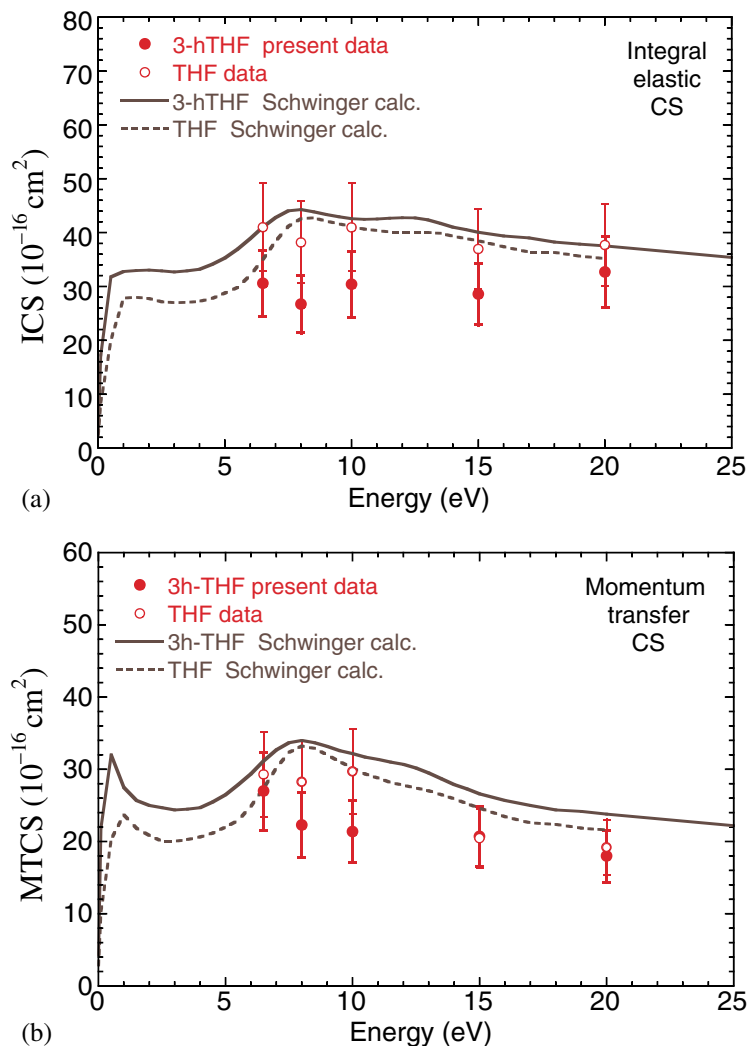


**Figure 4.** Present experimental and theoretical (a) ICS and (b) MTCS ( $10^{-16} \text{ cm}^2$ ). See legend on figure for further details.

energy mode) and the level of agreement between the two modes, while expected, gives further confidence in the accuracy of the procedures used.

#### 4.3. Integral and momentum transfer cross-section

The elastic integral cross-section (ICS) and the elastic momentum transfer cross-section (MTCS) are given at the foot of each column of table 1 and are presented in figures 4(a) and (b), respectively. These cross-sections have been derived from the present DCS measurements using a phase-shift analysis approach [27], which removes some of the subjectivity from the extrapolation process to those forward and backward angles not covered in the DCS measurements.

As might be expected, the integral cross-sections show the same trend as seen in the DCS, both between the experiment and the theory and between THF and 3-hTHF. The differences between the experimental ICS values for the two molecules are greater than those for the

momentum transfer cross-sections, reflecting the greater differences in the forward angle scattering behavior. In both the cases, the agreement with theory is acceptable. As in the case for THF, the shape resonance for 3-hTHF appears to be more prominent in the theoretical MTCS than in the ICS, reflecting the strong backscattering that occurs in the resonance region.

An analysis of the theoretical cross-sections and orbital plots for both THF and 3-hTHF leads to some tentative conclusions regarding the nature of the 6.5 eV resonance. The two lowest-lying empty valence orbitals in THF are largely C–O  $\sigma^*$  orbitals, but they also have significant density spread around the ring. If one assigns azimuthal quantum numbers to them in the simplest way (by counting radial nodes as one goes around the ring), they both look to be  $m = 4$ , and so are associated with angular momenta  $l \geq 4$ . This agrees with the results of Tonzani and Greene [11], who found through partial-wave analysis that the dominant partial wave in the THF resonance was  $l = 4$ . The broad resonance in the cross-section appears (on both chemical and symmetry-decomposition grounds) to be a superposition of shape resonances associated with trapping in these two orbitals, and the high-partial-wave contributions they bring in (on top of a low-partial-wave background, due to the relatively low energy) can therefore be expected to show up in the large-angle DCS. A similar situation occurs in cyclopropane, where there is an  $m = 3$  resonance at about 6 eV that creates observable structure in the DCS [28]–[31].

The situation that emerges is thus one where there is not just an overall enhancement of the high-angle DCS but one with some structure to it reflective of the leading partial wave (probably  $l = 4$ ) in the resonance orbitals. In particular, a maximum in the DCS at  $120^\circ$  grows in between 5 and 8 eV and then dies away again, so that the resonances stand out clearly there, whereas at  $180^\circ$  the DCS keeps rising monotonically out to 12 eV or so.

In 3-hTHF, the hydroxyl group complicates the picture, not only because of the lower symmetry but because the lowest empty orbitals spread out onto that group, and there is probably at least one additional shape resonance under the broad peak associated with it. But two of the three lowest virtual orbitals still look reasonably close to the lowest two in THF and the same basic picture regarding the resonance structure in the DCS could apply.

## 5. Conclusions

The present paper provides the first set of absolute DCS for elastic electron scattering from 3-hTHF, a molecule which is thought to provide a good analogue for the deoxyribose component of DNA. We find that at both the DCS and ICS levels, the experimental data and Schwinger variational calculations are in reasonably good agreement. The present results also indicate no major differences between the elastic scattering cross-sections for THF and 3-hTHF. However, the measured cross-sections for 3-hTHF are somewhat smaller than those for THF, while the calculations show the opposite trend. Further studies would thus be useful.

## Acknowledgments

This work is supported by the Australian Research Council. CW and VM acknowledge support by the Chemical Sciences, Geosciences and Biosciences Division, Office of Basic Energy Sciences, Office of Science, US Department of Energy, and use of the Jet Propulsion Laboratory's Supercomputing and Visualization Facility. It is a pleasure to acknowledge Laurie Campbell for the phase shift analysis of the DCS data and Darryl Jones for the Gaussian

calculations of the dipole moments and polarizabilities. It is also a pleasure to acknowledge helpful discussions with Gustavo Garcia and Paul Burrow.

## References

- [1] Boudaiffa B, Cloutier P, Hunting D, Huels M A and Sanche L 2000 *Science* **287** 1658
- [2] Aflatooni K, Scheer A M and Burrow P D 2006 *J. Chem. Phys.* **125** 054301
- [3] Zecca A, Perazzolli C and Brunger M J 2005 *J. Phys. B: At. Mol. Opt. Phys.* **38** 2079
- [4] Mozejko P, Ptasińska-Denga E, Domaracka A and Szmytkowski C 2006 *Phys. Rev. A* **74** 012708
- [5] Milosavljević A R, Giuliani A, Šević D, Hubin-Franskin M-J and Marinković B P 2005 *Eur. Phys. J. D* **35** 411
- [6] Coyle C J, Vizcaino V, Sullivan J P, Brunger M J and Buckman S J 2007 *New J. Phys.* **9** 41
- [7] Allan M 2007 *J. Phys. B: At. Mol. Opt. Phys.* **40** 3531
- [8] Winstead C and McKoy V 2006 *J. Chem. Phys.* **125** 074302
- [9] Trevisan C S, Orel A E and Rescigno T N 2006 *J. Phys. B: At. Mol. Opt. Phys.* **39** L255
- [10] Bouchiha D, Gorfinkiel J D, Caron L G and Sanche L 2006 *J. Phys. B: At. Mol. Opt. Phys.* **39** 975
- [11] Tonzani S and Greene C 2006 *J. Chem. Phys.* **125** 094504
- [12] Gibson J C, Morgan L A, Gulley R J, Brunger M J, Bundschu C T and Buckman S J 1996 *J. Phys. B: At. Mol. Opt. Phys.* **29** 3197
- [13] Gopalan A, Bommels J, Gotte B, Landwehr A, Franz K, Ruf M W, Hotop H and Bartschat K 2003 *Eur. Phys. J. D* **22** 17–29
- [14] Rohr K 1977 *J. Phys. B: At. Mol. Opt. Phys.* **10** 2215
- [15] Brunger M J and Buckman S J 2002 *Phys. Rep.* **357** 215
- [16] Nesbet R K 1979 *Phys. Rev. A* **20** 58
- [17] Boesten L and Tanaka H 1992 *At. Data Nucl. Data Tables* **52** 25
- [18] Schmidt M W *et al* 1993 *J. Comput. Chem.* **14** 1347
- [19] Berthier G, Cadioli B, Gallinella E, Aamouche A and Ghomi M 1997 *J. Mol. Struct. (Theochem)* **390** 11
- [20] Giardini A *et al* 2005 *ChemPhysChem* **6** 1164
- [21] Bauschlicher C W 1980 *J. Chem. Phys.* **72** 880
- [22] Takatsuka K and McKoy V 1981 *Phys. Rev. A* **24** 2473
- [23] Takatsuka K and McKoy V 1984 *Phys. Rev. A* **30** 1734
- [24] Winstead C and McKoy V 2000 *Comput. Phys. Commun.* **128** 386
- [25] Nelson R D, Lide D R and Margott A A 1967 Selected Values of Electric Dipole Moments for Molecules in the Gas Phase NSRDS-NBS10, Washington, DC
- [26] Lavrich R J, Rhea R L, McCargar J W and Tubergen M J 2000 *J. Mol. Spectrosc.* **199** 138
- [27] Campbell L, Brunger M J, Nolan A M, Kelly L J, Wedding A B, Harrison J, Teubner P J O, Cartwright D C and McLaughlin B 2001 *J. Phys. B: At. Mol. Opt. Phys.* **34** 1185
- [28] Winstead C, Sun Q and McKoy V 1992 *J. Chem. Phys.* **96** 4246
- [29] Allan M 1994 *Electron Collisions with Molecules, Clusters and Surfaces* ed H Ehrhardt and L A Morgan (New York: Plenum) p 105
- [30] Beyer T, Nestmann B M, Sarpal B K and Peyerimhoff S D 1997 *J. Phys. B: At. Mol. Opt. Phys.* **30** 3431
- [31] Čurík R and Gianturco F A 2002 *J. Phys. B: At. Mol. Opt. Phys.* **35** 717